# Data-Driven Probabilistic Methodology for Aircraft Conflict Detection Under Wind Uncertainty

**Jaime de la Mota**
**María Cerezo-Magaña**
**Alberto Olivares**
**Ernesto Staffetti**
Universidad Rey Juan Carlos, Madrid, Spain

***Abstract*— Assuming the availability of a reliable aircraft trajectory planner, this paper presents a probabilistic methodology to detect conflicts between aircraft, in the cruise phase of the flight, in the presence of wind prediction uncertainties quantified by ensemble weather forecasts, which are regarded as realizations of correlated random processes and employed to derive the eastward and northward components of the wind velocity. First, the Karhunen-Loève expansion is used to obtain a series expansion of the wind components in terms of a set of uncorrelated random variables and deterministic coefficients. Then, the uncertainty induced by these uncorrelated random variables in the outputs of the aircraft trajectory planner is quantified by means of the arbitrary polynomial chaos technique. Finally, the probability density function of the great circle distance between each pair of aircraft is derived from the polynomial expansions using a Gaussian kernel density estimator and employed to estimate the probability of conflict. The arbitrary polynomial chaos technique allows the effects of uncertainties in complex nonlinear dynamical system, such as those underlying aircraft trajectory planners, to be quantified with high computational efficiency, only requiring the existence of a finite number of statistical moments of the random variables of the Karhunen-Loève expansion, while avoiding any assumption on their probability distributions. In order to demonstrate the effectiveness of the proposed conflict detection method, numerical experiments are conducted through an optimal control based aircraft trajectory planner for a given wind forecast represented by an ensemble prediction system.**

***Index Terms*— Probabilistic Aircraft Conflict Detection, Ensemble Prediction Systems, Karhunen-Loève Expansion, Arbitrary Polynomial Chaos**

This work was supported in part by the Spanish Government under Grant TRA2017-91203-EXP and Grant RTI2018-098471-B-C33. E-mail: ernesto.staffetti@urjc.es. (Corresponding author: Ernesto Staffetti.)

Authors' address: Department of Telecommunication Engineering, Universidad Rey Juan Carlos, 28942 Madrid, Spain,



## I. INTRODUCTION

During the last decades, air traffic has grown at a steady rate. This growth has been affected by several crises. However, historic data show that commercial aviation has always recovered from them. To deal with the increase in air traffic, in 2005, the International Civil Aviation Organization (ICAO) proposed a new operational concept for Air Traffic Management (ATM) [1]. In the European Union, the Single European Sky ATM Research (SESAR) [2] is the ongoing program aimed to develop new ATM systems to better coordinate air traffic operations, thus increasing the efficiency, capacity, and safety of the current ATM system, while decreasing the environmental impact of commercial aviation. Similar programs are being developed in other countries, such as The Next Generation Air Transportation System (NextGen) [3], in the USA, and the Collaborative Actions for Renovation of Air Traffic Systems (CARATS), in Japan [4]. The main objective of the ATM is to ensure the safety of the flight.

A conflict among aircraft is one of the most dangerous situations in air traffic, which happens when the distance between two or more aircraft is smaller than the required minimum separation. More specifically, according to the current regulation [5], the horizontal separation distance should not be lower than 5 [NM], whereas the vertical separation should not be less than 1000 [ft].

Aircraft conflict avoidance systems operate in two stages, which are detection and resolution. In the detection stage, aircraft trajectories are predicted in the relevant airspace. Then, a conflict is detected when the probability of losing separation distance exceeds a certain threshold. In the resolution stage, selecting the most suitable manoeuvres, the predicted trajectories are modified in order to avoid the detected conflict. The sooner a conflict is detected, the more efficient Conflict Resolution (CR) manoeuvres can be performed in the resolution phase. Moreover, early Conflict Detection (CD) also reduces the workload of the air traffic controllers.

There are various sources of uncertainty that influence the accuracy of the aircraft trajectory prediction, such as data uncertainty, which appears when data are not exactly known, operational uncertainty, which originates in the lack of knowledge on the decisions taken by individuals, equipment uncertainty, which is associated with malfunctions and breakdowns of communication, navigation, and surveillance systems, and weather uncertainty, which appears when meteorological phenomena, mainly wind and thunderstorms, are not precisely predicted. Moreover, weather uncertainty affects the air traffic as a whole, thus having a very high influence on the accuracy of the trajectory prediction [6].

This paper investigates the aircraft CD problem in the presence of wind uncertainty. More specifically, the CD problem is studied in the cruise phase of the flight, in which probabilistic wind forecasts generated by Ensemble Prediction Systems (EPS) are employed to represent wind uncertainty.

Weather forecasts are estimates of the future state of the atmosphere. They are usually generated by estimating the initial conditions of the atmosphere using observations and then computing the temporal evolution of its state using a Numerical Weather Prediction (NWP) model. However, since these NWP models are very sensitive to the initial conditions, small errors in the initial state may result in large errors in the forecast. In EPS forecasts, the NWP model is run several times using slightly different initial conditions and model parameters, and then a set of forecasts is obtained, which is referred to as the ensemble. The individual forecasts of the ensemble are called members, which are assumed to be equiprobable. The differences between their corresponding initial states are consistent with the uncertainties in the observations. The goal of EPS, which typically are composed of between 10 and 50 members, is to represent the variety of states to which the atmosphere can evolve. Ideally, the future state of the atmosphere should be within the limit of the spread of the predicted ensemble. Further details on EPS can be found in [7], [8], [9].

The essence of the probabilistic approach to the aircraft CD problem is to estimate the separation distance loss probability between aircraft. The aircraft CD problem has been traditionally associated with the aircraft CR problem. Aircraft CD and Resolution (CD&R) methods can be classified, according to the look-ahead time at which they operate, into strategical, tactical, and operational, which operate with look-ahead times of more than 30 [min], between 30 and 10 [min], and less than 10 [min], respectively. A recent survey paper on aircraft CD&R is [10], which includes literature on aircraft CD in the presence of wind uncertainty. Another recent survey paper on stochastic modeling in aviation, which includes literature on aircraft CD in the presence of wind uncertainty, is [11].

In the aircraft CD problem, the aircraft trajectories are first predicted and then analyzed to calculate the probability of conflict between them. In particular, in the aircraft CD in which the wind forecast is represented by EPS, the uncertainty contained in the ensemble forecast has to be propagated to the prediction of the trajectories. There are two common approaches to trajectory prediction for CD using wind forecast generated by EPS: the transformation approach and the ensemble approach.

In the transformation approach, the probability distributions of the relevant uncertain meteorological parameters, such as the eastward and northward components of the wind velocity, are estimated from the ensemble forecast and, using a probabilistic trajectory planner, the probability distributions of the variables used to detect the conflict, such as the aircraft positions with respect to time, are obtained. In the ensemble approach, a deterministic trajectory planner is used to calculate a trajectory for each member of the ensemble wind forecast, thus obtaining an ensemble of trajectories, which is then employed to derive the probability distributions of the variables used to detect conflicts. Since it is less demanding from the computational point of view and provides similar results than the transformation approach [12], the ensemble approach is more suitable for practical applications.

In [13], a methodology to statistically quantify the severity of conflicts between aircraft flying at the same altitude, in the presence of wind forecast uncertainties derived from the PEARP EPS released by Météo-France, consisting of 35 members, is presented. The severity of the conflict is characterized by using two descriptors: conflict intensity and conflict probability. Conflict intensity is defined as the mean minimum distance between a pair of aircraft approaching a waypoint. The wind vector components are modeled as four-parameter beta distributions. The probability of conflict is obtained in terms of the Probability Density Function (PDF) of the minimum distance between aircraft, calculated from the PDFs of the wind components using the transformation approach, which allows the joint PDF of a set of random variables to be obtained from the joint PDF of another set of random variables. In [14], the aircraft CD methodology proposed in [13] is combined with a CR technique, in which conflicts between aircraft are solved, while minimizing the deviations from the original aircraft trajectories.

In [15], a methodology to compute the probability of conflict between aircraft flying 3D routes, in the presence of wind and temperature forecast uncertainties derived from the COSMO-D2 EPS released by the Deutscher Wetterdienst, consisting of 20-members, is presented. The ensemble approach is used, in which aircraft trajectories are calculated deterministically for each member of the ensemble and then, a deterministic CD method is conducted for all the computed trajectories. Since all the members are assumed to be equiprobable, the probability of conflict between each pair of aircraft is calculated as the fraction of members for which a conflict between these two aircraft is identified.

In [16], a multiple model method for aircraft conflict detection and resolution in the presence of intent and weather uncertainty, is proposed. It is based on probabilistic multiple model aircraft trajectory prediction. If a multiple model trajectory prediction is used, the separation vector between two aircraft has a Gaussian mixture distribution and an efficient randomized algorithm is proposed to estimate the conflict probability.

In [17], an efficient method for estimating the probability of conflict between aircraft is presented which is based on the so-called subset simulation technique, in which the small conflict probabilities are computed as a product of larger conditional conflict probabilities, reducing the computational cost and improving the accuracy of the probability estimation.

This paper presents a methodology to compute the probability of conflict between aircraft, flying at the same altitude, in the presence of wind prediction uncertainties quantified by ensemble weather forecasts. More specifically, the European Center for Medium-range Weather Forecast (ECMWF) EPS, consisting of 51 members, has been considered.

The eastward and northward components of the wind velocity have been modelled as two correlated random processes and the different members of the ensemble have been regarded as realisations of the two stochastic processes. The multiple uncorrelated Karhunen-Loève (muKL) expansion [18] has been applied to the ensemble to reduce the dimensionality of the representation of the two correlated random processes. The muKL expansion allows a set of uncorrelated random variables to be extracted, which encapsulate the uncertainty contained in the random processes. These random variables are the random inputs of the optimal control model used to generate the aircraft trajectories. The resulting model is a complex stochastic optimal control model, which is difficult to solve. Therefore, a surrogate model has been devised, which is computationally easier to solve and accurately approximates the propagation of the uncertainties, represented by the uncorrelated random variables, on the state variables of the solution of the optimal control problem. The state variables of this solution include the optimal trajectories of the aircraft. Polynomial Chaos Expansion (PCE) [19] has been used to formulate this surrogate model. PCE is a spectral method, which consists in the projection of the model outputs on a basis of orthogonal stochastic polynomials in the random inputs. This probabilistic method yields an efficient representation of the variability of the model outputs with respect to the variability of its inputs. In particular, in this paper, a data-driven moment-based PCE technique called arbitrary Polynomial Chaos (aPC) has been employed [20].

The Karhunen-Loève (KL) expansion is one of the most common approaches for dimension reduction in representing random processes as the infinite sum of orthogonal deterministic basis functions, called eigenfunctions, multiplied by uncorrelated random coefficients. This infinite sum can be truncated depending on the precision required in the representation of the random process. The KL expansion has been developed for a single random process or ensembles of statistically independent random processes and, therefore, its generalization to multi-correlated processes, namely to several random processes with mutual correlation, is not straightforward. Indeed, if the cross-covariances of several random processes are not zero, it is not easy to calculate consistent expansions for all the random processes that reflect both the structure of the autocorrelation and the structure of the cross-covariance. To overcome this difficulty, the muKL expansion has been introduced in [18]. The muKL expansion is a methodology that extends the classical KL expansion to multi-correlated nonstationary stochastic processes, which is based on the spectral decomposition of a suitable assembled random process and gives series expansions of the random processes using a single set of uncorrelated random variables.

The aPC expansion is a statistical moment-based PCE technique that allows surrogate models to be built. It extends the PCE techniques that require the knowledge of the PDF of the input random variables, such as the generalized polynomial chaos expansion [19]. Indeed, the aPC expansion only requires the existence of a finite number of moments of the input random variables of the model, which can be discrete or continuous and can be specified analytically as PDFs or numerically as histograms or raw data sets. This means that this polynomial expansion does not require the existence of a parametric PDF, avoiding the necessity to fit parametric probability distributions to data, which is very useful especially when a reduced amount of data is available.

In this paper, using the muKL expansion, the random processes that represent the components of the wind are approximated by a finite sum of the product of certain eigenfunctions multiplied by their corresponding uncorrelated random variables, which are characterized by using the aPC expansion. In the muKL expansion, the obtained uncorrelated random variables are ordered according to the amount of variability explained by each of them, which allows the truncation of the infinite sum to be carried out for a given precision. Then, the aPC expansion is calculated using the most significant random variables. A set of nodes and weights are computed in order to develop the surrogate models for the state variables of the optimal control model used to generate the aircraft trajectories, which represent the variability of the optimal trajectories of each aircraft. Finally, using the haversine formula, the marginal and joint PDFs of the distance between aircraft at each time instant are estimated, from which the aircraft conflict probabilities are computed.

This paper is organized as follows. Section II presents the general formulation of the muKL expansion, which allows for the dimension reduction of multi-correlated random processes. Section III describes the moment-based PCE technique, which permits the uncertainty quantification to be carried out. Section IV outlines the computational and statistical properties of the surrogate models represented by the PCE expansions, which are employed to estimate the marginal and joint PDFs of the distance between aircraft. The practical application of the proposed methodology for aircraft CD is shown in Section V. Finally, some conclusions are drawn in Section VI.

## II. Karhunen-Loève Expansion for Multi-correlated Random Processes

As mentioned before, the eastward and northward components of the wind forecast represented by the EPS are considered as realizations of correlated stochastic processes. Therefore, to implement their KL expansion, a specific methodology for correlated processes is employed. In particular, the muKL expansion is used, which is one of the two methodologies proposed in [18] with the aim to generalize the KL expansion in order to model multi-correlated non-stationary stochastic processes. The other approach is referred to as the Multiple Correlated KL (mcKL) expansion. The muKL technique has been chosen in this paper, since it allows the series expansions of the correlated processes to be generated in terms of a single set of uncorrelated random variables, whereas in the mcKL approach a different set of mutually correlated random variables must be developed for each process. In this section, the muKL method is described for convenience. A more in-depth treatment of the method accompanied by illustrative examples is given in [18].

Let $(\Omega, \Lambda, P)$ be a probability space, where $\Omega$ is the sample space, $\Lambda$ is a $\sigma$-algebra, and P is a probability measure. Consider the following ensemble of n zero-mean, square-integrable stochastic processes:

$$\{f_1(s;\omega), \dots, f_n(s;\omega))\}, \quad \omega \in \Omega. \tag{1}$$

Without loss of generality, it is assumed that all these processes are defined in the same bounded interval $[0, S]$, where index $s$ usually denotes time or space. More specifically, in this paper, index $s$ represents the spatial position in which weather data are predicted. Then, the correlation between the aforementioned processes is defined in terms of the following $n(n+1)/2$ covariance kernels:

$$C_{ij}(s_1, s_2) = E[f_i(s_1;\omega) f_j(s_2;\omega)], \;\; 1 \; \leq i \leq j \leq \; n, \tag{2}$$

where $E[\;\cdot\;]$ is the statistical expectation operator. In particular, $C_i(s_1, s_2) = C_{ii}(s_1, s_2)$ represents the autocovariance function of the process $f_i(s, \omega)$.

Notice that if the $n$ processes (1) are mutually independent, then the conventional KL expansion can be directly applied to each process, resulting in multiple series which can be built separately [21]. Conversely, if the cross-covariances (2) are not zero, then the classical KL expansion is not capable of providing consistent expansions for all the random processes, which reflect the autocorrelation and the cross covariance structure.

The muKL approach overcomes this drawback by generating a series expansion for each random process of the ensemble processes (1) in terms of a single set of uncorrelated random variables [22]. To obtain such a series, the following assembled process is defined:

$$\tilde{f}(s, \omega) = f_i(s - S_{i-1}; \omega), \quad s \in \mathcal{I}_i, \tag{3}$$

where $S_i = iS$ and $\mathcal{I}_i = (S_{i-1}, S_i], 1 \leq i \leq n$, with $\mathcal{I}_1 = [0, S_1]$. That is to say, the restriction of the assembled process $\tilde{f}(s, \omega)$ to the interval $\mathcal{I}_i$ corresponds to the process $f_i(s, \omega)$. Notice that $\tilde{f}(s, \omega)$ is a second-order process as well, which satisfies

$$E[\tilde{f}(s, \omega)] = 0, \;\; E[\tilde{f}(s_1, \omega)\tilde{f}(s_2, \omega)] = \tilde{C}(s_1, s_2),$$

where $\tilde{C}(s_1, s_2)$ is the assemble covariance function, which is defined as

$$\tilde{C}(s_1, s_2) = C_{ij}(s_1 - S_{i-1}, s_2 - S_{j-1}), \; s_1 \in \mathcal{I}_i, \;\; s_2 \in \mathcal{I}_j. \tag{4}$$

Then, a conventional KL expansion can be applied to the assembled process (3) obtaining

$$\tilde{f}(s, \omega) = \sum_{k=1}^{\infty} \sqrt{\lambda_k} \tilde{f}_k(s) \xi_k(\omega), \tag{5}$$

with $\xi_k(\omega)$ uncorrelated random variables, which are calculated as

$$\xi_k(\omega) = \frac{1}{\sqrt{\lambda_k}} \int_0^{S_n} \tilde{f}(s, \omega) \tilde{f}_k(s) ds,$$

with $\lambda_k$ and $\tilde{f}_k(s)$ defined as eigenvalues and eigenfunctions of a symmetric compact integral operator [23] whose kernel is (4), namely $\lambda_k$ and $\tilde{f}_k(s)$ are solutions to the following homogeneous Fredholm integral equation of the second kind:

$$\lambda_k \tilde{f}_k(s_1) = \int_0^{S_n} \tilde{C}(s_1, s_2) \tilde{f}_k(s_2) ds_2. \tag{6}$$

In practical applications, it is more convenient to work with non-negative covariance functions. Unfortunately, the assembled covariance $\tilde{C}(s_1, s_2)$ might have negative eigenvalues due to the fact that, in general, it is not positive semi-definite, even if all the covariances (2) are. Thus, a positivity condition for the assembled covariance $\tilde{C}(s_i, s_j)$ is imposed, that is to say

$$\sum_{j=1}^{m} \sum_{i=1}^{m} \tilde{C}(s_i, s_j) x_i x_j \geq 0,$$

for any finite sequence $\{s_1, \dots, s_m\}$ and any real numbers $x_i$, $i = 1, \dots, m$. Namely, the $m \times m$ matrix

$$\tilde{C} = \begin{bmatrix} \tilde{C}(s_1, s_1) & \tilde{C}(s_1, s_2) & \cdots & \tilde{C}(s_1, s_m) \\ \tilde{C}(s_2, s_1) & \tilde{C}(s_2, s_2) & \cdots & \tilde{C}(s_2, s_m) \\ \vdots & \vdots & \ddots & \vdots \\ \tilde{C}(s_m, s_1) & \tilde{C}(s_m, s_2) & \cdots & \tilde{C}(s_m, s_m) \end{bmatrix}$$

must be positive semi-definite for any collection of $m$ different values of $s \in [0, S]$.

Thus, the eigen-pairs $\{\lambda_k, \tilde{f}_k(s)\}, k = 1, 2, \dots,$ can be calculated and arranged according to the magnitudes of the eigenvalues $\lambda_k$ using (6). Moreover, each eigenfunction $\tilde{f}_k(s)$ can be expressed in terms of $n$ subfunctions $\phi_k^{(i)}(s), i = 1, \dots, n,$ which are defined as

$$\phi_k^{(i)}(s) = \tilde{f}_k(s + S_{i-1}) \mathcal{I}_{[0,S]}(s),$$

being $\mathcal{I}_{[0,S]}$ the indicator function in the interval $[0, S]$. Therefore, the $i$-th random process $f_i(s, \omega)$ of the original ensemble (1) is represented as follows:

$$f_i(s, \omega) = \sum_{k=1}^{\infty} \sqrt{\lambda_k} \phi_k^{(i)}(s) \xi_k(\omega). \tag{7}$$

Notice that the eigenvalues $\lambda_k$ and the random variables $\xi_k(\omega)$ which appear in (7), are the same as the ones introduced in (5). Moreover, for each index $i$, the collection of subfunctions $\{\phi_k^{(i)}(s)\}$, $k = 1, 2, \dots$ is neither orthogonal nor normalized in $s \in [0, S]$. Nevertheless, this drawback can be overcome by normalizing $\phi_k^{(i)}(s)$ within $[0, S]$, namely the random process $f_i(s, \omega)$ is rewritten as

$$f_i(s, \omega) = \sum_{k=1}^{\infty} \sqrt{\hat{\lambda}_k^{(i)}} \hat{\phi}_k^{(i)}(s) \xi_k(\omega), \tag{8}$$

being $\hat{\phi}_k^{(i)}(s) = \phi_k^{(i)}(s) / \left\| \phi_k^{(i)}(s) \right\|_2$ and $\hat{\lambda}_k^{(s)} = \lambda_k \left\| \phi_k^{(i)}(s) \right\|_2^2$.

For practical purposes, the dimensionality of the expansion (5) is reduced via truncation, and its associated mean-square error can be calculated. A truncated assembled process, which only considers the first $M$ elements of the expansion, is defined as follows:

$$Q_M(s,\omega) = \sum_{k=1}^{M} \sqrt{\lambda_k}\tilde{f}_k(s)\xi_k(\omega), \tag{9}$$

whereas the associated mean-squared error is calculated as

$$\varepsilon_M^2 = \int_0^{S_n} E[(\tilde{f}(s,\omega) - Q_M(s,\omega))^2]ds. \tag{10}$$

Taking into account that $\xi_k(\omega)$ are uncorrelated random variables and $\tilde{f}_k(s)$ are orthonormal eigenfunctions, the mean-squared error (10) can be expressed as

$$\varepsilon_M^2 = \sum_{k=M+1}^{\infty} \lambda_k. \tag{11}$$

Thus, the truncation error of the series expansion (5) decreases with respect to the decay rate of the eigenvalues. Furthermore, the mean-squared error (10) is an upper bound on the truncation error of the series expansion (8), whereas the errors of the cross-covarances $C_{ij}(s_1,s_2)$ are bounded by the error of the assembled covariance $\tilde{C}(s_1,s_2)$ defined in (4).

In practical applications, a key aspect of any KL expansion is the election of the appropriate number of terms in the truncated expansion. In particular, in the muKL expansion, a threshold for the error $\varepsilon_M$ can be imposed to determine the choice of $M$ in (9). According to (11), this can be achieved by imposing a threshold on the relative sum of eigenvalues, as follows:

$$\sum_{k=1}^{M} \lambda_k \geq \delta \sum_{k=1}^{\infty} \lambda_k,$$

being $\delta \in [0,1]$ an arbitrary constant chosen so that the accuracy of the approximation is satisfactory for a particular application.

Notice that, in order to incorporate the muKL expansion into the aircraft trajectory planner model, the eigenfunctions $\phi_k^{(i)}(s), i = 1,\ldots,n$, associated to the expansions of the eastward and northward components of the wind velocity must be interpolated to be converted into analytic expressions. Moreover, the uncertainty of the corresponding random variables $\xi_k(\omega)$ must be quantified, which can be done using the aPC expansion introduced in Section III.

## III. Moment-Based Arbitrary Polynomial Chaos

This section introduces the aPC approach, which is employed in this article to represent the propagation of the uncertainties through the aircraft trajectory planner model. A more complete description of this methodology can be found in [20].

Let $\boldsymbol{\xi} = (\xi_1,\xi_2,\ldots,\xi_{N_U})$ be a vector of $N_U$ independent random variables in the probability space $(\Omega,\Lambda,P)$ introduced in Section II. Notice that, for the sake of simplicity, the formal dependency on $\omega$ is dropped for $\xi_i(\omega), i = 1,\ldots,N_U$. Then, a surrogate model for each output variable $x(t,\boldsymbol{\xi})$ of the aircraft trajectory planner can be computed, which is represented by a multidimensional polynomial expansion. In particular, a linear combination of $N_P$ stochastic multivariate orthonormal polynomials $\boldsymbol{\Psi}_k(\boldsymbol{\xi})$ with deterministic coefficients $\alpha_k(t)$ can be used to approximate the output variable $x(t,\boldsymbol{\xi})$ as follows:

$$\begin{aligned} x(t,\boldsymbol{\xi}) = x(t;\xi_1,\xi_2,\ldots,\xi_{N_U},) \approx \\ \sum_{k=1}^{N_P} \alpha_k(t)\boldsymbol{\Psi}_k(\xi_1,\xi_2,\ldots,\xi_{N_U}). \end{aligned} \tag{12}$$

In (12), the multivariate orthonormal polynomials $\boldsymbol{\Psi}_k(\boldsymbol{\xi})$, with $1 \leq k \leq N_P$, are calculated as the product of univariate orthonormal polynomials $\psi_j^i(\xi_i)$, with $1 \leq i \leq N_U$, $1 \leq j \leq p$, where $i$ indicates the elements of the vector of random variables and $j$ the order of the univariate orthonormal polynomials. As a consequence of the orthonormality of the polynomials, the $N_P$ coefficients $\alpha_k(t)$ introduced in (12) can be calculated as follows:

$$\alpha_k(t) = \int_{\boldsymbol{\xi}\in\Omega} x(t,\boldsymbol{\xi})\boldsymbol{\Psi}(\boldsymbol{\xi})dP(\boldsymbol{\xi}). \tag{13}$$

In particular, in this article, a Gaussian quadrature rule based on the statistical moments of $\boldsymbol{\xi} = (\xi_1,\xi_2,\ldots,\xi_{N_U})$ is employed to solve (13). For a given multivariate function $\mathcal{F}(\boldsymbol{\xi})$, the full tensor product quadrature formula $\mathcal{F}(\boldsymbol{\xi})$ can be written as

$$\begin{aligned} \int_{c_1}^{d_1} \cdots \int_{c_{N_U}}^{d_{N_U}} \mathcal{F}(\boldsymbol{\xi}) \approx \\ \sum_{i_1=1}^{p_1} \cdots \sum_{i_{N_U}=1}^{p_{N_U}} \mathcal{F}(\zeta^{i_1},\ldots,\zeta^{i_{N_U}})(w_{i_1} \otimes \cdots \otimes w_{i_{N_U}}), \end{aligned} \tag{14}$$

being $\zeta^{i_j}$ and $w_{i_j}$, $1 \leq i \leq N_U$, $1 \leq j \leq p$, respectively, the nodes and weights of the numerical integration, which are obtained from the statistical moments of the random variables $\boldsymbol{\xi} = (\xi_1,\xi_2,\ldots,\xi_{N_U})$ [20].

Therefore, the statistical moments of the random variables of the aircraft trajectory planner model are employed to determine the optimal nodes and weights of the surrogate model, as well as the corresponding orthonormal polynomials. Thus, the aPC approach offers a general framework, which permits to handle both random variables with known parametric distributions and data sets with unknown parametric distributions [24].

## IV. Uncertainty Quantification

The polynomial expansion (12) provides a computationally efficient way to obtain the mean and variance of the output variables $x(t,\boldsymbol{\xi})$ of the aircraft trajectory planner model using the coefficients $\alpha_k(t)$. Specifically,

$$\begin{aligned} \mu_x &= \alpha_1(t), \\ \sigma_x^2 &= \sum_{k=2}^{N_P} \alpha_k^2(t). \end{aligned}$$

Moreover, according to the quadrature rule defined in (14), the mean and variance can be easily calculated in terms of scalar products as:

$$\begin{aligned}\mu_x &= x(t;\zeta^{i_1},\ldots,\zeta^{i_{N_U}})\cdot \boldsymbol{w},\\ \sigma_x^2 &= (x(t;\zeta^{i_1},\ldots,\zeta^{i_{N_U}})-\mu_x)^2\cdot \boldsymbol{w},\end{aligned}$$

being $\boldsymbol{w} = (w_{i_1},\ldots,w_{i_{N_U}})$, $1 \le i \le p$, the vector of Gaussian quadrature weights.

The polynomial expansion (12) also allows the PDFs of the output variables of the aircraft trajectory planner model to be estimated at each time instant. More specifically, a kernel density estimation approach can be used, which is based on the formulation of a data smoothing problem [25]. Then, given a safety threshold, the marginal and joint PDFs of the output variables can be employed to estimate the separation distance loss probability between aircraft along their whole trajectories.

## V. Application

To demonstrate the effectiveness of the probabilistic methodology for aircraft CD proposed in this paper, a numerical experiment has been conducted. In this experiment, a conflict scenario involving three aircraft has been considered, in which the trajectory of each aircraft is predicted and, given a safety threshold, the separation distance loss probability between each pair of aircraft is estimated. This probability is calculated, at each time instant, from the PDFs of the distance between aircraft.

More specifically, an optimal control based aircraft trajectory planner is considered, in which precise models of the aircraft are formulated. The use of accurate aircraft dynamic models is required in order to improve the predictability of the trajectories and obtain realistic estimates. To solve the optimal control problems, a numerical pseudospectral knotting method is employed. In particular, both the aircraft model used and the numerical resolution method applied are those described in [26]. Thus, the distances between pairs of aircraft involved in the CD problems, as well as their corresponding PDFs, are derived from the optimal state variables obtained in the solution of these optimal control problems.

In the considered scenario, the three aircraft, denoted as Aircraft A, Aircraft B, and Aircraft C, are assumed to be flying at cruise level. The latitudes and longitudes of their initial positions are indicated in Table I. The specific time at which the aircraft are located at these initial positions is March 19, 2022 at 06:00 UTC, which will be referred to as the initial time of the experiment. Their trajectories are predicted using the aforementioned optimal control based aircraft trajectory planner, in which the objective functional considered is the final time, namely it has been assumed that the aircraft must reach their final positions in minimum time. The latitudes and longitudes of the final positions of each aircraft are also given in Table I. A representation of this scenario along with the initial and final positions of the aircraft are shown in Figure 1. More specifically, as shown in the instrumental chart of the Spanish upper airspace represented in Figure 1, the Aircraft A follows Airway `UN871`, Aircraft B follows Airway `UN873` and, after reaching the VOR/DME `GDV` of Gran Canaria switches to Airway `UN858`, and Aircraft C follows Airway `UN729`.

TABLE I: Initial and final positions of Aircraft A, Aircraft B, and Aircraft C.

| | Units | Aircraft A | Aircraft B | Aircraft C |
|---|---|---|---|---|
| Initial latitude $\phi_I$ | [deg] | 25.869 N | 25.283 N | 25.147 N |
| Final latitude $\phi_F$ | [deg] | 28.505 N | 28.689 N | 28.746 N |
| Initial longitude $\lambda_I$ | [deg] | $-18.389$ E | $-17.428$ E | $-14.964$ E |
| Final longitude $\lambda_F$ | [deg] | $-14.677$ E | $-14.967$ E | $-15.547$ E |

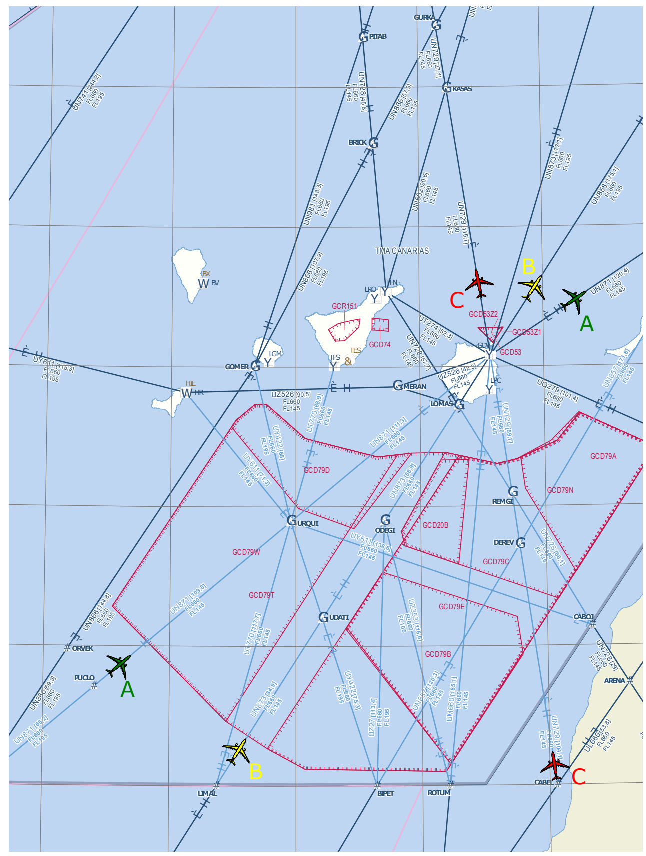


Fig. 1: Inital and final positions of the three aircraft considered in the numerical experiment. Aircraft A, B, and C are represented in green, yellow, and red colours, respectively.

As mentioned in Section I, to predict the aircraft trajectories, wind data obtained from the 50-member ECMWF EPS have been used. The default eastward and northward components of the wind velocity of each member of the ECMWF EPS forecast are provided at a regular latitude-longitude grid, with a spatial resolution from 0.5 to 3 [deg], at 9 atmospheric levels corresponding to different pressure levels from 1000 to 50 [hPa]. Custom spatial resolutions can also be selected. The temporal coverage is 6 hour data two times daily.

In this paper, the chosen pressure level is 200 [hPa], which corresponds to the cruise altitude and the selected spatial resolution is $0.5 \times 0.5$ [deg]. Moreover, a series of equally-weighted forecasts with different time horizons have been used. Specifically, the predictions published on March 19, 2022 at 00:00 with time horizon 06 [h], March 18, 2022 at 12:00 with time horizon 18 [h], March 18, 2022 at 00:00 with time horizon 30 [h], March 17, 2022 at 12:00 with time horizon 42 [h], March 17, 2022 at 10:00 with time horizon 54 [h], and on March,16 2022 at 12:00 with time horizon 66 [h]. Therefore, a total of 300 members of these ensambles have been employed whose forecasts coincide with the initial time of the experiment. The mean and standard deviation, measured in [m/s], of the eastward and northward components of the wind velocity, obtained from these 300 ensemble members, are shown in Figures 2 and 3, respectively.

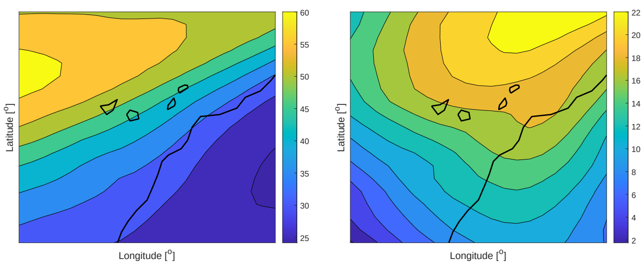


(a) Eastward component. (b) Northward component.

Fig. 2: Mean value, in [m/s], of the magnitude of the components of the wind velocity calculated using ECMWF EPS forecasts for March 19, 2022 at 6:00 for the pressure altitude 200 [hPa].

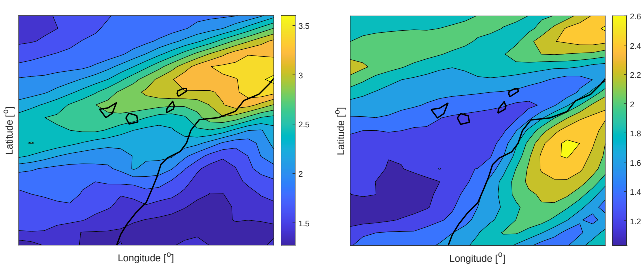


(a) Eastward component. (b) Northward component.

Fig. 3: Standard deviation, in [m/s], of the magnitude of the components of the wind velocity calculated using ECMWF EPS forecasts for March 19, 2022 at 6:00 for the pressure altitude 200 [hPa].

Therefore, the muKL expansion of the wind velocity components has been computed using 300 realizations of the stochastic process. In particular, a truncated muKL expansion, represented by Equation (9), with $M = 4$ has been considered. The percentages of variability explanation by each random variable of the expansion are reported in Table II.

As already mentioned in Section II, to include the wind velocity information in the aircraft trajectory planner model, an analytic function that interpolates the eigenfunctions of the wind velocity components derived from the muKL expansion must be determined. More specifically, in this paper, a Radial Basis Functions (RBF) based interpolation method is employed. The RBF is a widespread technique that allows multidimensional data to be interpolated, which can be gridded or scattered, namely the RBF can deal with both structured and unstructured data [27].

TABLE II: Percentages of explanation of each random variable of the muKL expansion.

| Random variable | % of explanation |
|---|---|
| $\xi_1(\omega)$ | 29.394 |
| $\xi_2(\omega)$ | 17.930 |
| $\xi_3(\omega)$ | 13.079 |
| $\xi_4(\omega)$ | 8.610 |
| Total | 69.013 |

Once the aircraft trajectories are predicted using the optimal control based aircraft trajectory planner, the corresponding optimal state variables are employed to calculate both the main statistics and the PDFs of the distance between each pair of aircraft at each time instant. More specifically, the orthodromic distance between aircraft is computed from the obtained optimal latitudes and longitudes using the haversine formula.

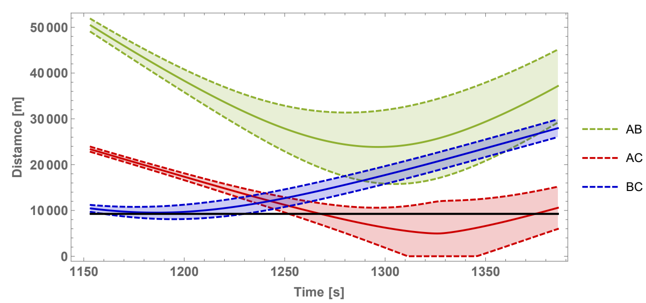


Fig. 4: Mean distance between each pair of aircraft together with the corresponding 2-sigma uncertainty envelopes. The horizontal solid black line represents a distance of 5 [NM], the minimum separation required.

Figure 4 shows the mean distances between each pair of aircraft together with their associated 2-sigma confidence envelopes calculated using the proposed CD probabilistic methodology. The black horizontal line represents the minimum separation distance between aircraft required by the current regulation, namely 5 [NM] [5]. It can be seen in Figure 4 that, based on the 2-sigma confidence envelope criterion, conflicts between Aircraft A and Aircraft C and between Aircraft B and Aircraft C are detected, whereas no conflict between Aircraft A and Aircraft B is indicated. Moreover, the same conclusion is obtained if a 3-sigma confidence envelope criterion is used.

The vertical grey segments depicted in Figure 5 represent five time instants, namely $1235.08$ [s], $1265.88$ [s],

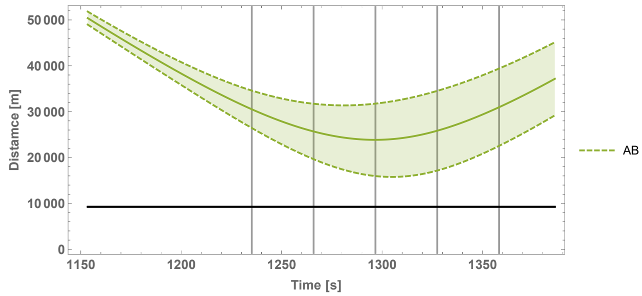


Fig. 5: Mean distance between Aircraft A and Aircraft B together with the corresponding 2-sigma uncertainty envelope. The vertical segments in grey represent five time instants, namely $1235.08$ [s], $1265.88$ [s], $1296.68$ [s], $1327.48$ [s], and $1358.28$ [s], at which the PDF of the distance between these aircraft is calculated and shown in Figure 6. The horizontal solid black line represents a distance of 5 [NM], the minimum separation required.

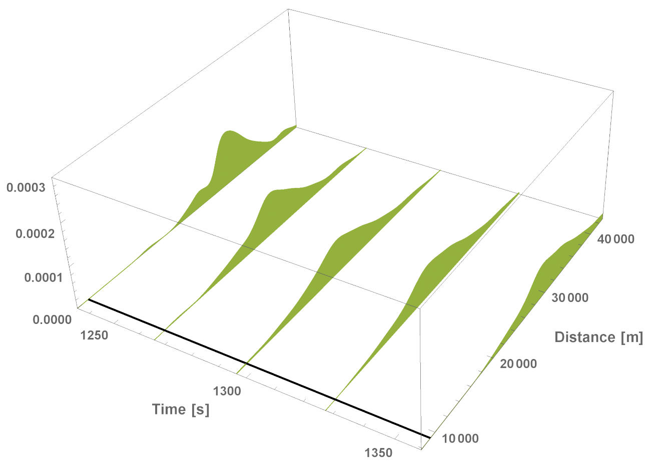


Fig. 6: PDFs of the distance between Aircraft A and Aircraft B at time instants $1235.08$ [s], $1265.88$ [s], $1296.68$ [s], $1327.48$ [s], and $1358.28$ [s]. The solid black line represents a distance of 5 [NM], the minimum separation required.

$1296.68$ [s], $1327.48$ [s], and $1358.28$ [s], at which the PDFs of the distances between Aircraft A and Aircraft B have been estimated. The resulting PDFs are shown in Figure 6. At the point of closest distance, which occurs at time $1296.68$ [s], the probability of conflict is $0.0085$, which is a significant value from the air traffic safety point of view. Thus, it can be concluded that, unlike the CD criterion based on the the 2-sigma confidence envelope, the CD criterion based on the probability is able to detect a conflict between Aircraft A and Aircraft B.

The surrogate model (12) allows not only the marginal PDF of the distance between two aircraft at any time instant to be calculated but also the joint PDF of the distances between two aircraft in correspondence with two different time instants to be computed. As an example, the joint PDF of the distances between Aircraft A and Aircraft B, at times $1296.68$ [s] and $1199.66$ [s], is

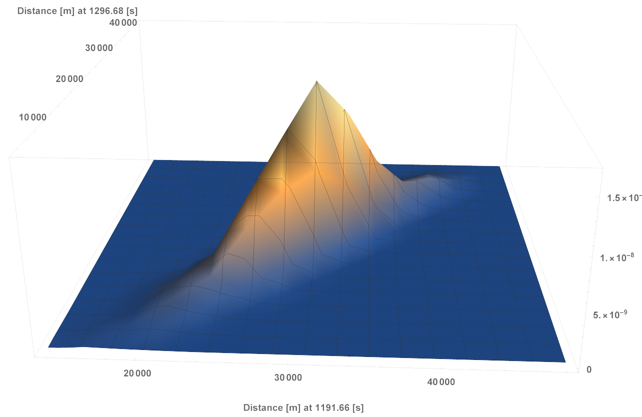


(a) Joint PDF.

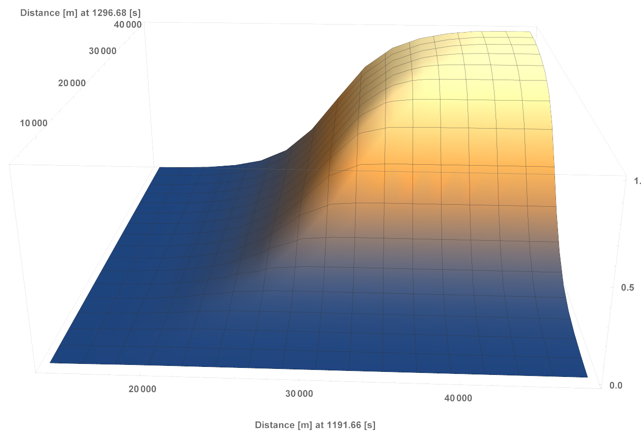


(b) Joint CDF.

Fig. 7: Joint PDF and joint CDF of the distances between Aircraft A and Aircraft B at times $1296.68$ [s] and $1199.66$ [s].

represented in Figure 7.a, whereas the corresponding joint CDF is shown in Figure 7.b. From this joint probability distribution it is possible to calculate both joint and conditional probabilities of conflict. For instance, knowing that the distance between Aircraft A and Aircraft B at time $1199.66$ [s] is higher than 25 [NM], the probability of conflict at time $1296.68$ [s] conditioned by this event becomes $4.89 \cdot 10^{-16}$, which is considerably lower than the marginal probability 0.0085.

## VI. Conclusions

In this paper, a probabilistic approach to aircraft conflict detection in the cruise phase of flight in the presence of wind prediction uncertainty quantified by an ensemble weather forecast has been proposed. Specifically, a conflict among aircraft has been assumed to happen when the distance between two or more aircraft is smaller than the required minimum separation.

To this purpose, the multiple uncorrelated Karhunen-Loève expansion, the arbitrary polynomial chaos expansion, and a Gaussian kernel density estimator have been combined with a deterministic trajectory planner to quantify the uncertainty associated to the northward and eastward components of the wind velocity and obtain the probability density function of the distance between aircraft at different time instants, which allows the probability of conflict between pairs of aircraft to be calculated. The joint probability density function of the distance between two aircraft at two different time instants has also been estimated, which permits joint and conditional probabilities of conflict between pairs of aircraft to be computed.

The ensemble prediction system provided by the European Centre for Medium-Range Weather Forecast has been employed in this paper as the probabilistic wind forecast, whereas a deterministic aircraft trajectory planner based on pseudospectral optimal control has been used to generate the aircraft trajectories. However, the proposed data-driven probabilistic methodology for aircraft conflict detection is a general approach in which any ensemble prediction system and any deterministic aircraft trajectory planner can be employed.

In the numerical experiments, the proposed methodology has been applied to detect conflicts among aircraft flying at cruise altitude. More specifically, conflicts between aircraft have been detected not only by calculating the marginal probability of occurrence at a certain time instant but also computing the conditional probability of occurrence, in which the conditioning event is assumed to be information about the distance between the two aircraft at a previous time instant. As expected, information about the distance between two aircraft at a certain previous time instant has a great influence on the probability of conflict between the same aircraft at a future time instant. Moreover, it has been proven that this approach to conflict detection based on the probability of occurrence is much more accurate than the approach based on confidence envelopes of the separation between aircraft, which, from the safety point of view, is a key aspect for the air traffic management system.

The proposed methodology represents a new framework to expand the capabilities of current aircraft conflict detection systems in the presence of uncertainty on wind velocity, since it is able of yielding marginal and conditional probabilities of conflict and not only confidence intervals.

## REFERENCES


[1] A. Andreeva-Mori, S. Suzuki, and E. Itoh, “Rule derivation for arrival aircraft sequencing,” Aerospace Science and Technology, vol. 30, no. 1, pp. 200–209, 2013.

[2] Joint Undertaking, “European ATM master plan, 2015 edition,” Brussels, Belgium: EUROCONTROL, 2015.

[3] Joint Planning and Development Office, “Concept of operations for the next generation air transportation system, Ver. 3.2,” https://apps.dtic.mil/sti/pdfs/ADA535795.pdf, 2010.

[4] Japan Civil Aviation Bureau, “Long-term vision for the future air traffic systems (CARATS),” https://www.mlit.go.jp/common/000128185.pdf, 2010.

[5] International Civil Aviation Organization, “Procedures for air navigation services,” Air traffic management, no. 4444, 2016.

[6] A. Cook and D. Rivas, Complexity Science in Air Traffic Management. Routledge, 2016.

[7] T. Palmer, “The ECMWF ensemble prediction system: Looking back (more than) 25 years and projecting forward 25 years,” Quarterly Journal of the Royal Meteorological Society, vol. 145, pp. 12–24, 2019.

[8] R. Buizza, P. Houtekamer, G. Pellerin, Z. Toth, Y. Zhu, and M. Wei, “A comparison of the ECMWF, MSC, and NCEP global ensemble prediction systems,” Monthly Weather Review, vol. 133, no. 5, pp. 1076–1097, 2005.

[9] F. Molteni, R. Buizza, T. N. Palmer, and T. Petroliagis, “The ECMWF ensemble prediction system: Methodology and validation,” Quarterly Journal of the Royal Meteorological Society, vol. 122, no. 529, pp. 73–119, 1996.

[10] J. Tang, “Conflict detection and resolution for civil aviation: A literature survey,” IEEE Aerospace and Electronic Systems Magazine, vol. 34, no. 10, pp. 20–35, 2019.

[11] R. Shone, K. Glazebrook, and K. G. Zografos, “Applications of stochastic modeling in air traffic management: Methods, challenges and opportunities for solving air traffic problems under uncertainty,” European Journal of Operational Research, vol. 292, no. 1, pp. 1–26, 2021.

[12] D. Rivas, A. Franco, and A. Valenzuela, “Analysis of aircraft trajectory uncertainty using ensemble weather forecasts,” in Proc. 7th European Conference for Aeronautics and Space Sciences. Milan, Italy, July 3-6, 2017.

[13] E. Hernandez-Romero, A. Valenzuela, and D. Rivas, “A probabilistic approach to measure aircraft conflict severity considering wind forecast uncertainty,” Aerospace Science and Technology, vol. 86, pp. 401–414, 2019.

[14] E. Hernández-Romero, A. Valenzuela, and D. Rivas, “Probabilistic multi-aircraft conflict detection and resolution considering wind forecast uncertainty,” Aerospace Science and Technology, vol. 105, p. 105973, 2020.

[15] E. Hernández-Romero, “Probabilistic aircraft conflict detection and resolution under the effects of weather uncertainty,” Ph.D. dissertation, Universidad de Sevilla, 2020.

[16] V. P. Jilkov, J. H. Ledet, and X. R. Li, “Multiple model method for aircraft conflict detection and resolution in intent and weather uncertainty,” IEEE Transactions on Aerospace and Electronic Systems, vol. 55, no. 2, pp. 1004–1020, 2018.

[17] C. Mishra, S. Maskell, S.-K. Au, and J. F. Ralph, “Efficient estimation of probability of conflict between air traffic using subset simulation,” IEEE Transactions on Aerospace and Electronic Systems, vol. 55, no. 6, pp. 2719–2742, dec 2019.

[18] H. Cho, D. Venturi, and G. Karniadakis, “Karhunen–Loève expansion for multi-correlated stochastic processes,” Probabilistic Engineering Mechanics, vol. 34, pp. 157–167, 2013.

[19] D. Xiu, Numerical Methods for Stochastic Computations: A Spectral Method Approach. Princeton University Press, 2010.

[20] R. Ahlfeld, B. Belkouchi, and F. Montomoli, “SAMBA: Sparse approximation of moment-based arbitrary polynomial chaos,” Journal of Computational Physics., vol. 320, pp. 1–16, 2016.

[21] S. Huang, S. Quek, and K. Phoon, “Convergence study of the truncated Karhunen–Loève expansion for simulation of stochastic processes,” International Journal for Numerical Methods in Engineering, vol. 52, no. 9, pp. 1029–1043, 2001.

[22] J. Ramsay and B. Silverman, Applied Functional Data Analysis. Springer, 2002.

[23] T. Kato, Perturbation Theory for Linear Operators. Springer Science & Business Media, 2013.

[24] S. Oladyshkin and W. Nowak, “Data-driven uncertainty quantification using the arbitrary polynomial chaos expansion,” Reliability Engineering & System Safety, vol. 106, pp. 179–190, 2012.

[25] A. Gramacki, Nonparametric Kernel Density Estimation and its Computational Aspects. Springer, 2018.

[26] M. Cerezo-Magaña, A. Olivares, and E. Staffetti, “Formation mission design for commercial aircraft using switched optimal con-

trol techniques," IEEE Transactions on Aerospace and Electronic Systems, vol. 57, no. 4, pp. 2540–2557, 2021.
[27] M. D. Buhmann, Radial Basis Functions: Theory and Implementations. Cambridge University Press, 2003.